Tohoku J. Exp. Med., 2023, **260**, 181-191

Effects of *Ndufs4* Deletion on Hearing after Various Acoustic Exposures

Tomotaka Hemmi,[1,*] Jun Suzuki,[1,*] Yoshiteru Kagawa,[2] Yohei Honkura,[1] Ryoukichi Ikeda,[3] Ken Hashimoto,[1] Chitose Suzuki,[4] Tetsuaki Kawase,[1,5] Takaaki Abe,[4] Yuji Owada[2] and Yukio Katori[1]

[1]Department of Otolaryngology-Head and Neck Surgery, Tohoku University Graduate School of Medicine, Sendai, Miyagi, Japan
[2]Department of Organ Anatomy, Tohoku University Graduate School of Medicine, Sendai, Miyagi, Japan
[3]Department of Otolaryngology, Head and Neck Surgery, Iwate Medical University School of Medicine, Shiwa-gun, Iwate, Japan
[4]Department of Clinical Biology and Hormonal Regulation, Tohoku University Graduate School of Medicine, Sendai, Miyagi, Japan
[5]Laboratory of Rehabilitative Auditory Science, Tohoku University Graduate School of Biomedical Engineering, Sendai, Miyagi, Japan

Mitochondrial dysfunction can cause cochlear dysfunction and accelerate noise-induced hearing loss (NIHL). NADH dehydrogenase (ubiquinone) Fe-S protein 4 (Ndufs4) is one of the subunits of mitochondrial complex I and has a role in the assembly and stabilization of complex I. However, the involvement of Ndufs4 in the pathogenesis of NIHL has not been reported. The aim of this study was to evaluate whether *Ndufs4* deletion causes vulnerability to noise exposures. The wild-type (WT) and *Ndufs4* knockout (KO) mice with C57BL/6J genetic background were used. Cochlear histology and hearing thresholds were assessed after noise exposure at 100 or 86 dB sound pressure level (SPL). Immunostaining showed the widespread expression of Ndufs4 in the cochlea. After noise exposure at 100 dB SPL, auditory brainstem response (ABR) threshold shifts at 4 kHz in *Ndufs4* KO mice were significantly higher than that in WT mice. After noise exposure at 86 dB SPL, ABR threshold shifts, wave 1 amplitudes, and the number of synapses in the inner hair cells were not significantly different. RNA sequencing revealed the decreased expression of energy generation-related genes in *Ndufs4* KO mice. *Ndufs4* deficiency accelerates permanent low-frequency threshold shifts after moderate noise exposure.

Keywords: hair cell; mitochondrial dysfunction; Ndufs4; noise-induced hearing loss; synapse
Tohoku J. Exp. Med., 2023 July, **260** (3), 181-191.
doi: 10.1620/tjem.2023.J031

Introduction

Mitochondrial dysfunction induced by genetic abnormalities or oxidative damage causes cochlear tissue deterioration, resulting in sensorineural hearing loss, such as age-related hearing loss and noise-induced hearing loss (NIHL) (Hott et al. 2003; Someya and Prolla 2010; Fujimoto and Yamasoba 2014, 2019). NIHL, particularly hearing loss resulting in a permanent threshold shift (PTS), is caused by moderate to severe noise exposure that increases reactive oxygen species production in cochlear lymph fluids and tissues, including the hair cells and stria vascularis (Ohlemiller et al. 1999; Yamashita et al. 2004). One of its suggested pathophysiologies is mitochondria-mediated apoptosis in outer hair cells (OHCs) (Tuerdi et al. 2017). However, the complicated relationship between mitochondrial dysfunction and NIHL is still unclear.

Since Kujawa and Liberman (2009) reported that mild noise exposure that causes temporal threshold shift (TTS) could induce permanent loss of inner hair cells (IHCs) and

Received February 16, 2023; revised and accepted April 10, 2023; J-STAGE Advance online publication April 20, 2023
*These two authors contributed equally to this work.
Correspondence: Jun Suzuki, Department of Otolaryngology-Head and Neck Surgery, Tohoku University Graduate School of Medicine, 1-1 Seiryo-machi, Aoba-ku, Sendai, Miyagi 980-8574, Japan.
e-mail: j_suzuki1212@orl.med.tohoku.ac.jp

spiral ganglion neuron (SGN) synapses (cochlear synaptopathy), this type of NIHL has been a growing concern as a hidden hearing loss and hearing impairment without audiogram change (Schaette and McAlpine 2011; Liberman et al. 2015; Liberman 2017; Liberman and Kujawa 2017). IHC-SGN synapses, not OHCs, are the most vulnerable to noise exposure (Liberman 2017). Moreover, glutamate excitotoxicity is known to be the primary pathophysiology of cochlear synaptopathy (Ruel et al. 2007; Liberman and Kujawa 2017). However, it is still unknown whether mitochondrial dysfunction contributes to the pathogenesis of cochlear synaptopathy.

NADH dehydrogenase (ubiquinone) Fe-S protein 4 (Ndufs4) is one of the subunits of mitochondrial complex I (NADH: ubiquinone oxidoreductase), the first enzyme of the mitochondrial electron transport chain, and it has a role in the assembly and stabilization of complex I (Sterky and Larsson 2008; Ingraham et al. 2009; Shil et al. 2021). Mutation of human *NDUFS4* is associated with Leigh syndrome, an early-onset, progressive neurodegenerative disorder characterized by psychomotor regression, seizures, and early death due to respiratory failure (Ortigoza-Escobar et al. 2016). Owing to encephalomyopathy, conventional *Ndufs4* knockout (KO) mice similarly show retarded growth, weight loss, motor dysfunction, respiratory abnormalities, and premature death around 7 weeks of age (Kruse et al. 2008; Quintana et al. 2010). Recent studies evaluating various neuron-specific *Ndufs4* conditional KO mice have shown that loss of *Ndufs4* in neurons might be a critical factor in encephalopathy development (Chen et al. 2017; Bolea et al. 2019; Shil et al. 2021). Furthermore, *Ndufs4* deficiency decreased expression of synaptophysin, a presynaptic protein, in the hippocampus (Shil et al. 2021). A genome-wide association study in mice using auditory brainstem response (ABR) wave 1 amplitude suggested that *Ndufs4* might be related to the susceptibility to noise-induced cochlear synaptopathy (Lavinsky et al. 2018). Although it can be inferred from these past reports that *Ndufs4* contributes to the pathophysiology of NIHL, including both PTS and TTS, it has not yet been fully investigated. In this study, we explored whether *Ndufs4* deletion causes vulnerability to noise exposures using conventional *Ndufs4* KO mice.

Materials and Methods

Animals and experimental protocol

Male and female wild-type (WT) and *Ndufs4* KO mice with C57BL/6J genetic background (B6.129S4-Ndufs4$^{tm1.1Rpa}$/J) were used in this study (4 weeks of age, weighing 8-15 g at study onset). Because our preliminary experiments showed that *Ndufs4* KO mice exhibit early-onset progressive hearing loss as early as 6 weeks of age and premature death around 7 weeks of age, we decided to use mice aged 4 to 6 weeks for these experiments to avoid the effect of progressive hearing loss. Heterozygous *Ndufs4* KO mice were crossed, and their offspring were genotyped through polymerase chain reaction (PCR) with the following primers to obtain WT and homozygous *Ndufs4* KO mice: *Ndufs4* common forward (5′-GAGC TTGCCTAGGAGGAGGT-3′), *Ndufs4* WT reverse (5′-AGTCAGCAACATTTTGGCAGT-3′), and *Ndufs4* mutant reverse (5′-AGGGGACTGGACTAACAGCA-3′). The following cycling conditions were used: 94°C for 2 min, 10 cycles of 94°C for 20 s, 65°C for 15 s, and 68°C for 10 s, 28 cycles of 94°C for 15 s, 60°C for 15 s, and 72°C for 10 s, followed by 72°C for 2 min and 4°C indefinitely. PCR products were separated on a 2.0% agarose gel to detect bands with the following expected sizes: 201 bp for WT and 400 bp for *Ndufs4* mutant alleles. Throughout the experiment, the mice were housed in a 12 h light-dark cycle at a constant temperature with food and water available ad libitum. All mice were treated following the guidelines presented in the Standards for Human Care and Use of Laboratory Animals of Tohoku University, Guidelines for Proper Conduct of Animal Experiments by the Ministry of Education, Culture, Sports, Science, and Technology of Japan, and the National Institute of Health Guide for the Care and Use of Laboratory Animals. All the animal experiments were approved by the Ethics Committee for Animal Experiments of Tohoku University Graduate School of Medicine (2019-249).

The mice were divided into three experimental groups (Fig. 1A). In group 1, seven male WT mice and seven male *Ndufs4* KO mice were assigned and sampled on postnatal (P) day 32 (P32). Three mice were used for surface preparations and paraffin sections in both WT and *Ndufs4* KO groups, and four mice were used for RNA sequencing. In group 2, five female WT mice and five female *Ndufs4* KO mice were assigned and subjected to 100 dB acoustic exposure on P34. Subsequently, ABR thresholds were measured 2 days before and 1 and 8 days after acoustic exposure. After the sampling on P42, the left cochlea was used for surface preparation, and the right was used for paraffin sections. In group 3, six male WT mice and six male *Ndufs4* KO mice were assigned and subjected to 86 dB acoustic exposure on P34. Afterward, the same process as described above was performed.

Hearing function test

The ABR threshold was measured as described previously (Suzuki et al. 2020). The mice were anesthetized using ketamine (100 mg/kg body weight) and xylazine (20 mg/kg body weight) through intraperitoneal administration. Needle electrodes were placed subcutaneously at the vertex (active electrode), base of the ear pinna (reference electrode), and back (ground electrode). ABR recordings were performed using a TDT System 3 auditory-evoked potential workstation and BioSigRP software (Tucker-Davis Technologies, Alachua, FL, USA). ABR responses were evoked using bursts of pure tones at frequencies of 4, 8, 12, 16, and 32 kHz. Evoked responses were averaged across 1,000 sweeps. Responses were collected for stimulus levels

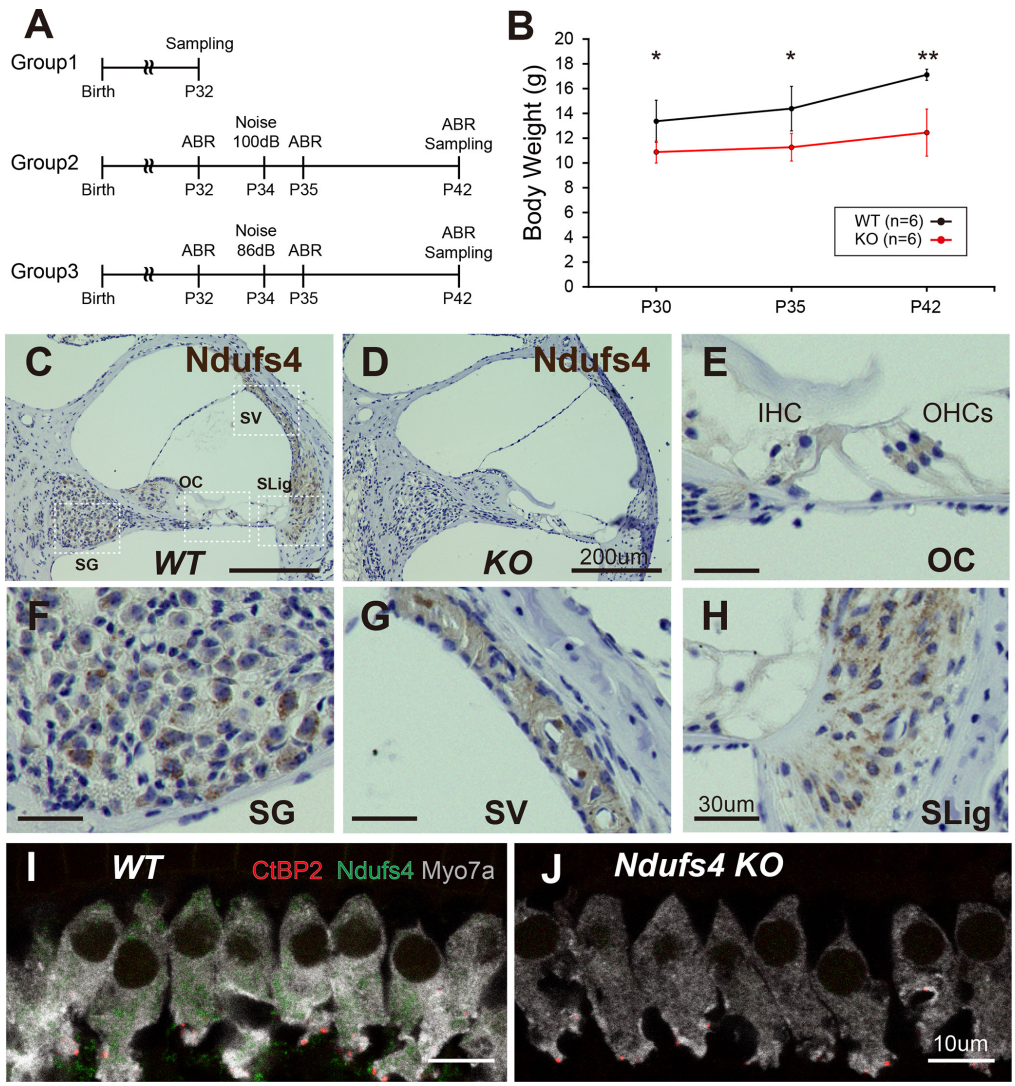

Fig. 1. Experimental groups, body weights, and Ndufs4 expression in the cochlea.
Wild-type (WT) and *Ndufs4* knockout (KO) mice were divided into three groups: seven male WT mice and seven male *Ndufs4* KO mice in group 1, five female WT mice and five female *Ndufs4* KO mice in group 2, and six male WT mice and six male *Ndufs4* KO mice in group 3 (A). The body weights of male *Ndufs4* KO mice were significantly lower than those of male WT mice (B). The expression of Ndufs4 in the cochleae of WT mice was confirmed at the organ of Corti (OC), spiral ganglion (SG), stria vascularis (SV), and spiral ligament (SLig) (C, E-H), but not in *Ndufs4* KO mice (D). Ndufs4 was distributed in the cytoplasm of the inner hair cells of WT mice (I), but not in *Ndufs4* KO mice (J). Scale bars represent 200 μm (C and D), 30 μm (E-H), and 10 μm (I and J). Statistical significance was determined by two-way repeated measures analysis of variance, followed by a Šídák multiple comparison test. *P < 0.05; **P < 0.01. Error bars represent the standard deviation.

in 5 dB steps from 100 dB sound pressure level (SPL) to 10 dB SPL. The measurement of ABR and determination of the threshold were performed by separate examiners. The ABR threshold was defined as the lowest SPL at which a recognizable waveform could be detected. If a mouse showed no response, the stimulus threshold was defined as 105 dB SPL. The ABR wave 1 amplitude was determined as the average of the voltage difference between the highest positive and lowest negative values for the first wave at 80, 90, and 100 dB SPL.

Noise exposure

Awake and unrestrained mice were placed in individual sections of a wire-mesh cage and were exposed to an 8-16 kHz octave-band noise at 86 or 100 dB SPL for 2 h as previously described (Honkura et al. 2016). The sound was generated by a waveform generator (SF-06, Random Noise Generator; RION, Tokyo, Japan), amplified (D-75A, Crown, Northridge, CA, USA), filtered (Multifunction Filter, NF Corporation, Austin, TX, USA), and presented in an open field by a dome tweeter (2446H, JBL, Northridge, CA, USA) positioned at the center of the cage. The sound level was measured using a sound level meter (2250L,

Brüel & Kjær, London, UK)

Tissue preparation

Mice were deeply anesthetized with an intraperitoneal injection of ketamine (100 mg/kg) and xylazine (20 mg/kg) and transcardially perfused with 10% formalin neutral buffer solution (pH 7.4) (Wako, Osaka, Japan). The inner ears were quickly dissected from the skull and immediately soaked in a 10% formalin neutral buffer solution. Small holes were made at the round and oval windows and apex of the cochleae. The cochleae were perfused through the cochlear scalae, post-fixed with 10% formalin neutral buffer solution at 4°C overnight, and decalcified in 10% ethylenediaminetetraacetic acid for 2 days at room temperature.

Cochlear histology using coronal sections

To detect the difference of cochlear histological damage, paraffin sections (3 μm) were stained with hematoxylin and eosin (H&E) and observed under a microscope (BZ-9000, Keyence, Osaka, Japan) separately in the apical, middle, and basal turns. The cell density of SGNs and the thickness of the SV within each turn were calculated. The area and cell numbers were determined using BZ-H1C software (Keyence). Cell density was calculated by dividing the total number of cells by the area measured and expressed as the number of cells per mm^2.

Cochlear wholemount and hair cell counts

After fixation and demineralization as discussed above, surface preparations of the left cochlea were processed as previously described (Honkura et al. 2019). The hair cells were stained for F-actin with rhodamine-conjugated phalloidin (1:100, Rhodamine Phalloidin, Thermo Fisher Scientific, Waltham, MA, USA) for 1 h at room temperature under light-protected conditions. Low-power fluorescence images were obtained using a microscope (BZ-9000, Keyence) and BZ-H1C software (Keyence), and the full-length cochlea image was assembled and analyzed in Adobe Photoshop CS6 (San Jose, CA, USA). An ImageJ plug-in (https://meeeplfiles.partners.org/Measure_line.class) was used to create a cochlear frequency map. Damaged and undamaged IHCs and OHCs were counted in the seven frequency-specific regions (4.0, 8.0, 11.3, 16.0, 22.6, 32.0, and 45.2 kHz) of the cochlea.

Ndufs4 immunostaining of cochlear sections

The cochlea was prepared using a procedure similar to that used for other histological analyses; however, glyoxal (ALTIFiX, Falmam, Tokyo, Japan) was used as fixing solution. The decalcified cochleae were embedded in paraffin, and 3 μm coronal sections were made. After deparaffinization, antigen retrieval was conducted by autoclaving for 5 min at 120°C using an antigen-activating solution (1:10, #415211, Nichirei, Tokyo, Japan). Immunohistochemistry with anti-Ndufs4 antibody was performed using a Histofine® mouse stain kit (#424021, Nichirei). Tissue sections were blocked using a blocking reagent A (#424021, Nichirei) for 1 h at room temperature and incubated overnight with a primary antibody (anti-Ndufs4, a mouse monoclonal IgG2a κ, 1:50, #sc-100567, Santa Cruz Biotechnology, Dallas, CA, USA) at 4°C. Endogenous peroxidase was removed using methanol and 30% H_2O_2, then the sections were processed using reagent B (#424021, Nichirei) for 10 min at room temperature and simple stain mouse MAX-PO (M) (#424021, Nichirei) for 20 min at room temperature. Subsequently, the sections were incubated with peroxidase-conjugated streptavidin, and 3,3′-diaminobenzidine substrate was added. Hematoxylin was used for counterstaining.

Immunostaining of cochlear wholemount

After fixation and demineralization as discussed above, surface preparations of the cochlea were processed. Glyoxal was used as fixing solution for Ndufs4 immunostaining. Immunohistochemistry of cochlear wholemount was processed as previously described with modifications (Suzuki et al. 2016). The samples were permeabilized by freezing in 30% sucrose, blocked for 1 h at room temperature in phosphate-buffered saline with 0.03% Triton X and 3% bovine serum albumin, and washed with phosphate-buffered saline. The tissue was then incubated overnight at 37°C with the following primary antibodies: (1) mouse isotype IgG1 anti-C-terminal binding protein 2 (CtBP2, 1:200, #612044, BD Transduction Laboratories, Franklin Lakes, NJ, USA), (2) mouse isotype IgG2 anti-glutamate receptor 2 (GluA2, 1:2000, #MAB397, Millipore, Burlington, MA, USA), and (3) rabbit anti-myosin VIIa (Myo7a, 1:200, #25-6790, Proteus BioSciences, Ramona, CA, USA). After rinsing, the tissue was incubated for 1 h at 37°C in the following secondary antibodies: (1) goat anti-mouse IgG1 Alexa Fluor 568 conjugate (1:1,000, #A-21124, Thermo Fisher Scientific), (2) goat anti-mouse IgG2a Alexa Fluor 488 conjugate (1:1,000, #A-21131, Thermo Fisher Scientific), and (3) chicken anti-rabbit Alexa Fluor 647 (1:200, #A-21443, Thermo Fisher Scientific). Mouse monoclonal IgG2 anti-Ndufs4 (1:50, #sc-100567, Santa Cruz Biotechnology) was used instead of anti-GluA2 to evaluate the expression of Ndufs4 in hair cells. Low-power fluorescence images were obtained using a microscope (BZ-9000, Keyence) and BZ-H1C software (Keyence), and the full-length cochlea image was assembled and analyzed.

Synapse count

A confocal microscope (TCS SP8, Leica Microsystems, Wetzlar, Germany) fitted with a 63 × objective and 2.4 × digital zoom was used in the imaging of the cochlear wholemounts at frequency locations of 11.3, 16, 22.6, 32, and 45.2 kHz with a z-step increment of 0.25 μm. Imaging of each frequency location was performed in two adjacent regions for a total of approximately 20 IHCs per frequency location. Maximum intensity projection images were created using an image processing software (Leica

Application Suite X, Leica Microsystems) to identify and measure presynaptic ribbons and postsynaptic glutamate receptor patches. The number of functional synapses (CtBP2 signals merged with GluA2 signals) was counted and expressed as functional synapses per total number of IHCs in a maximum-intensity projection image. The number of IHCs in a maximum intensity projection image was counted using the CtBP2 (to stain the nuclei) and myosin VIIa antibodies (to stain the cytoplasm). The images were merged using Adobe Photoshop CS6.

RNA extraction and RNA sequencing

The inner ears were quickly dissected from the skull and stored at −80°C. RNA extraction from the cochleae was performed using RNAiso Plus (Cat# 9180, Takara Bio, Kusatsu, Japan) according to the manufacturer's instructions. The total RNA of the mice was extracted using RNAiso Blood (Cat# 9112, Takara Bio) according to the manufacturer's instructions. The RNA pellets were dissolved in 30 μL Milli-Q Water (Merck Millipore, Burlington, MA, USA), and the RNA solutions of eight samples (WT: n = 4 and *Ndufs4* KO: n = 4) were checked for integrity using an Agilent RNA 600 Nano Kit (Cat# 5067-1511, Agilent Technologies, Santa Clara, CA, USA) on a Bioanalyzer (Agilent Technologies). The RNA Integrity Number of all samples was ≥ 7.2, which means that the RNA of all samples could be subjected to library preparations for total RNA sequencing. Subsequently, 500 ng of RNA was used from each sample to create libraries using NEBNext Ultra II RNA Library Prep Kit for Illumina and NEBNext rRNA Depletion Kit v2 (Cat# E7770S and E7400L, New England Biolabs, Ipswich, MA, USA) according to the manufacturer's instructions. The final PCR cycle was 14. The concentrations and size distributions of the libraries were measured using an Agilent DNA 7500 kit (Cat#5067-1506, Agilent Technologies) with a Bioanalyzer. All samples were analyzed using next-generation sequencing (NGS) equipment. The libraries were pooled, and the concentrations were adjusted to 1 nM. The pooled libraries were subjected to denaturation and neutralization. Subsequently, the libraries were diluted to 1.8 pM and applied for an NGS run using NextSeq500/550 v2.5 (75 Cycles) kits (Cat#20024906, Illumina, San Diego, CA, USA) in the NextSeq 500 System (Illumina). The sequencing was performed with paired-end reads of 36 bases. After the sequencing run, FASTQ files were exported, and the basic information of the NGS run data was checked on CLC Genomics Workbench 20.0.3 software (QIAGEN, Hilden, Germany). In the quality assessment of the reads, a PHRED score > 20 was confirmed for 99.97% of all reads, indicating the success of the run.

Bioinformatics analysis

Average reads per kilobase of exon per million mapped reads of > 0.5 and P-values <0.01 were regarded as differentially expressed genes (DEGs) and uploaded to Metascape (https://metascape.org/gp/index.html#/main/step1), which is an open online analysis software that can perform pathway and process enrichment analysis based on numerous ontology sources (Zhou et al. 2019).

Statistical analysis

Statistical analyses were conducted using Prism 9 (GraphPad Software, San Diego, CA, USA) for two-way or two-way repeated measures analysis of variance, followed by a Šídák multiple comparison test. All data are presented as means ± standard deviation. Statistical significance was set at $P < 0.05$.

Results

Time course of body weights

WT and *Ndufs4* KO mice were weighed on P30, P35, and P42 to evaluate the effect of *Ndufs4* deletion on body weight during this experiment. The body weights of *Ndufs4* KO mice were significantly lower than those of WT mice at each time point during the experiment (Fig. 1B).

Ndufs4 localization and expression in adult mouse cochleae

Immunohistochemistry was performed using paraffin sections and wholemount cochleae to confirm that Ndufs4 protein is localized in the mouse cochlea (Fig. 1C) and that *Ndufs4* KO mice lack Ndufs4 protein expression (Fig. 1D). In WT mice on P32, cochlear coronal section images showed broad expression of Ndufs4 throughout the cochlea: the expression of Ndufs4 was confirmed in the organ of Corti, spiral ganglia, stria vascularis (SV), and spiral ligaments in WT mice (Fig. 1C, E-H), but not in *Ndufs4* KO mice (Fig. 1D). IHCs and OHCs in the organ of Corti; SGNs in the spiral ganglia; marginal, intermediate, and basal cells in the SV; and fibrocytes in spiral ligaments showed Ndufs4 expression in their cytoplasm (Fig. 1E-H). No apparent signal differences in Ndufs4 expression were observed among each cochlear turn. Moreover, it was also confirmed that Ndufs4 was distributed in the cytoplasm of IHCs of WT mice using cochlear wholemounts (Fig. 1I), but not in *Ndufs4* KO mice (Fig. 1J). These results showed that Ndufs4 protein is broadly localized in the mouse cochlea, and that *Ndufs4* KO mice lack Ndufs4 protein expression.

Ndufs4 deletion causes deterioration of low-tone hearing after noise exposure

Cochlear function and histology were examined after exposure to an 8-16 kHz octave-band noise at 100 dB SPL for 2 h to evaluate the effects of *Ndufs4* deletion on noise exposure that causes moderate PTS (~50 dB SPL). The baseline ABR thresholds were not different between WT and *Ndufs4* KO mice (Fig. 2A). Eight days after noise exposure, the ABR thresholds of both WT and *Ndufs4* KO mice were significantly elevated at all frequencies except 4 kHz in WT mice (Fig. 2A). ABR threshold shifts at 4 kHz of *Ndufs4* KO mice were significantly higher than that of

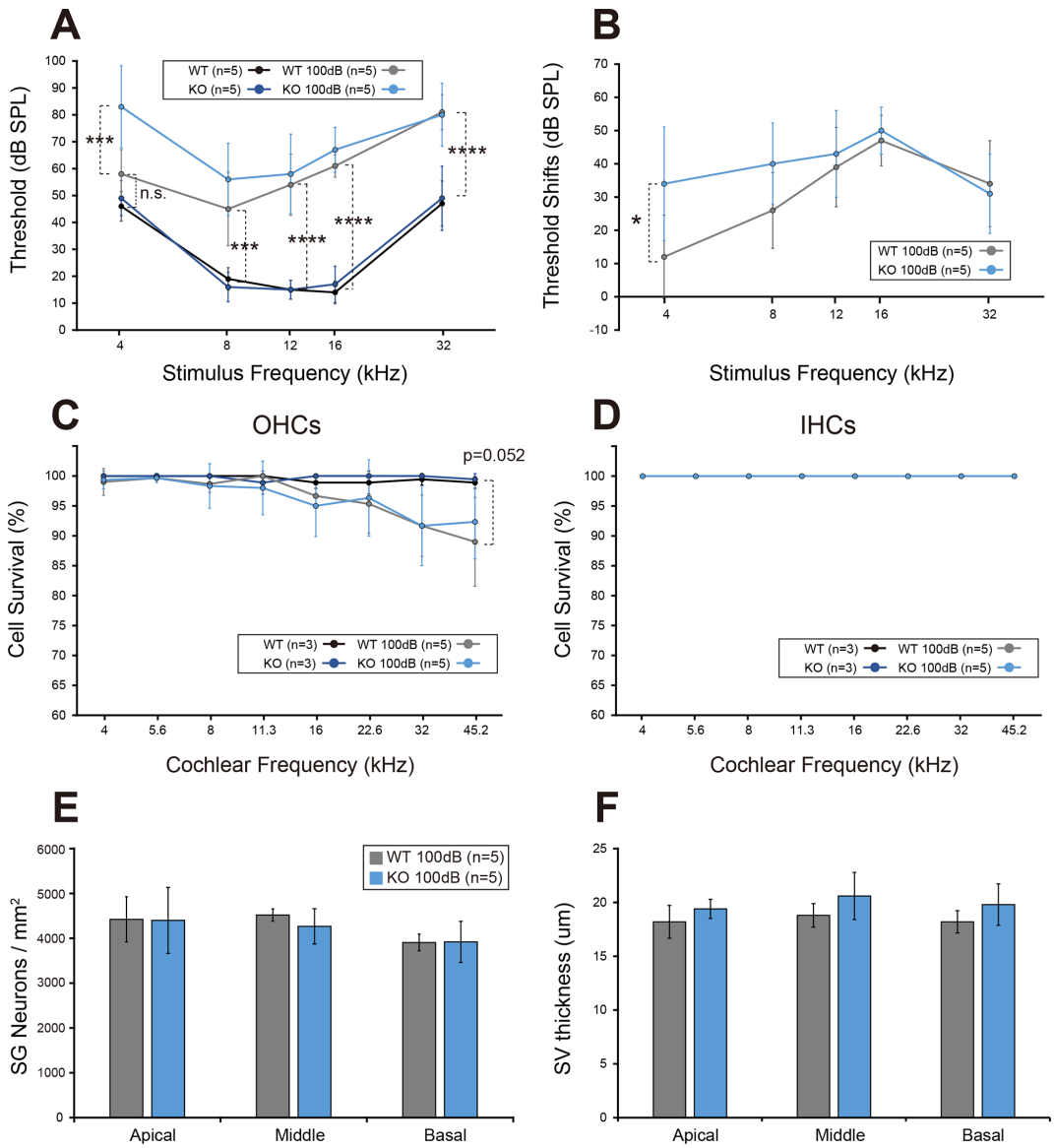

Fig. 2. Noise-induced hearing loss after moderate noise exposure.
Eight days after 100 dB noise exposure, the auditory brainstem response (ABR) thresholds of both wild-type (WT) and *Ndufs4* knockout (KO) mice were significantly elevated at all frequencies except 4 kHz in WT mice (A). ABR threshold shifts at 4 kHz in *Ndufs4* KO mice were significantly higher than in WT mice (B). No significant differences between WT and *Ndufs4* KO mice after noise exposure in outer hair cell (OHC) and inner hair cell (IHC) survival, spiral ganglion (SG) neuron survival, and stria vascularis (SV) thickness (C-F). Statistical significance was determined by two-way analysis of variance, followed by a Šídák multiple comparison test. n.s., not significant. *P < 0.05; ***P < 0.001; ****P < 0.0001. Error bars represent the standard deviation.

WT mice (Fig. 2B). These results suggest that *Ndufs4* deletion causes deterioration of low-tone hearing after noise exposure.

Subsequently, histological examinations were performed using cochlear paraffin sections (Supplementary Fig. S1A-D) and cochlear wholemounts (Supplementary Fig. S1E-F). No apparent endolymphatic hydrops was observed in apical turn of WT and *Ndufs4* KO mice. Quantitative analyses did not reveal any significant differences between WT and *Ndufs4* KO mice after noise exposure in OHC, IHC, and SGN survival and SV thickness (Fig. 2C-F).

Ndufs4 deletion does not accelerate synapse loss after noise exposure

WT and *Ndufs4* KO mice were exposed to an 8-16 kHz octave-band noise at 86 SPL for 2 h to investigate the effects of *Ndufs4* deletion on IHC synapse damage after noise exposure. The baseline ABR thresholds were not different between WT and *Ndufs4* KO mice (Fig. 3A). Eight days after noise exposure, the ABR thresholds of both WT and *Ndufs4* KO mice were significantly elevated at 16 kHz

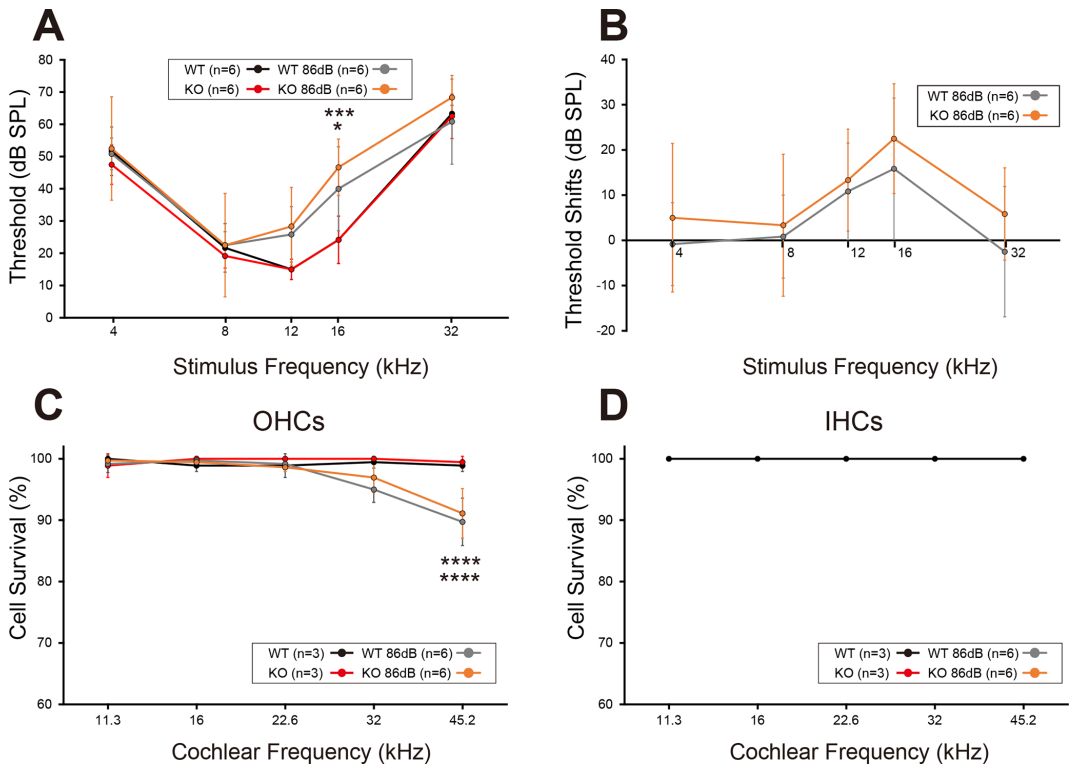

Fig. 3. Noise-induced hearing loss after mild noise exposure.
Eight days after 86 dB noise exposure, the auditory brainstem response (ABR) thresholds of both wild-type (WT) and *Ndufs4* knockout (KO) mice were significantly elevated at 16 kHz (A), but ABR threshold shifts were not significantly different between WT and *Ndufs4* KO mice (B). Significant decreases in outer hair cell (OHC) survival after noise exposure in WT and *Ndufs4* KO mice at the 45.2 kHz region (C). No significant differences between WT and *Ndufs4* KO mice in OHC and inner hair cell (IHC) survival (C-D). Statistical significance was determined by two-way analysis of variance, followed by a Šídák multiple comparison test. *P < 0.05; ***P < 0.001; ****P < 0.0001. Error bars represent the standard deviation.

(Fig. 3A); however, ABR threshold shifts were not significantly different between WT and *Ndufs4* KO mice (Fig. 3B). These results suggest that 86 dB noise exposure causes mild PTS (~25 dB), and *Ndufs4* deletion does not cause hearing deterioration after noise exposure at this noise level. Histological analyses showed a significant loss of OHCs at the 45.2 kHz region in both WT and *Ndufs4* KO mice (Fig. 3C). There were no significant differences between WT and *Ndufs4* KO mice after noise exposure in OHC survival (Fig. 3C) and IHC survival (Fig. 3D), which corresponds to the physiological results.

Subsequently, the number of IHC ribbons (CtBP2 signals) and functional synapses (CtBP2 signal with GluA2 signal) was counted using cochlear wholemount images taken by confocal microscopy (Fig. 4A-D). Quantitative analyses revealed that 86 dB noise exposure causes significant loss of functional synapses at the 32 and 45.2 kHz regions. However, there were still no significant differences between WT and *Ndufs4* KO mice (Fig. 4E). Correspondingly, the ABR wave 1 amplitudes were also attenuated at the 8, 12, and 16 kHz regions in both groups 8 days after noise exposure; however, there were no significant differences between WT and *Ndufs4* KO mice (Fig. 4F). These results collectively suggest that *Ndufs4* deletion has no apparent effect on synaptic damage after noise exposure both histologically and physiologically.

Screening for DEGs in the WT and Ndufs4 KO mouse cochleae

The changes in gene expression between WT and *Ndufs4* KO mice at 4 weeks of age were examined using RNA sequencing analysis to reveal the function of *Ndufs4* in the mouse cochlea. The read number was approximately 27 to 35 million per sample as paired-end reads. A total of 17 genes were chosen as up-regulated DEGs and 30 genes were chosen as down-regulated DEGs in the cochlea of *Ndufs4* KO mouse (Supplementary Tables S1 and S2).

Bioinformatics analysis of DEGs in the WT and Ndufs4 KO mouse cochleae

The functional annotation and pathway enrichment analysis of 17 up-regulated DEGs and 30 down-regulated DEGs were carried out using Metascape (Supplementary Fig. S2). In down-regulated DEGs, “generation of precursor metabolites and energy” was the significant enriched term in the category (Table 1). It can be inferred from these results that the ability of mitochondria to generate precursor metabolites and energy is impaired in the cochlea of *Ndufs4*

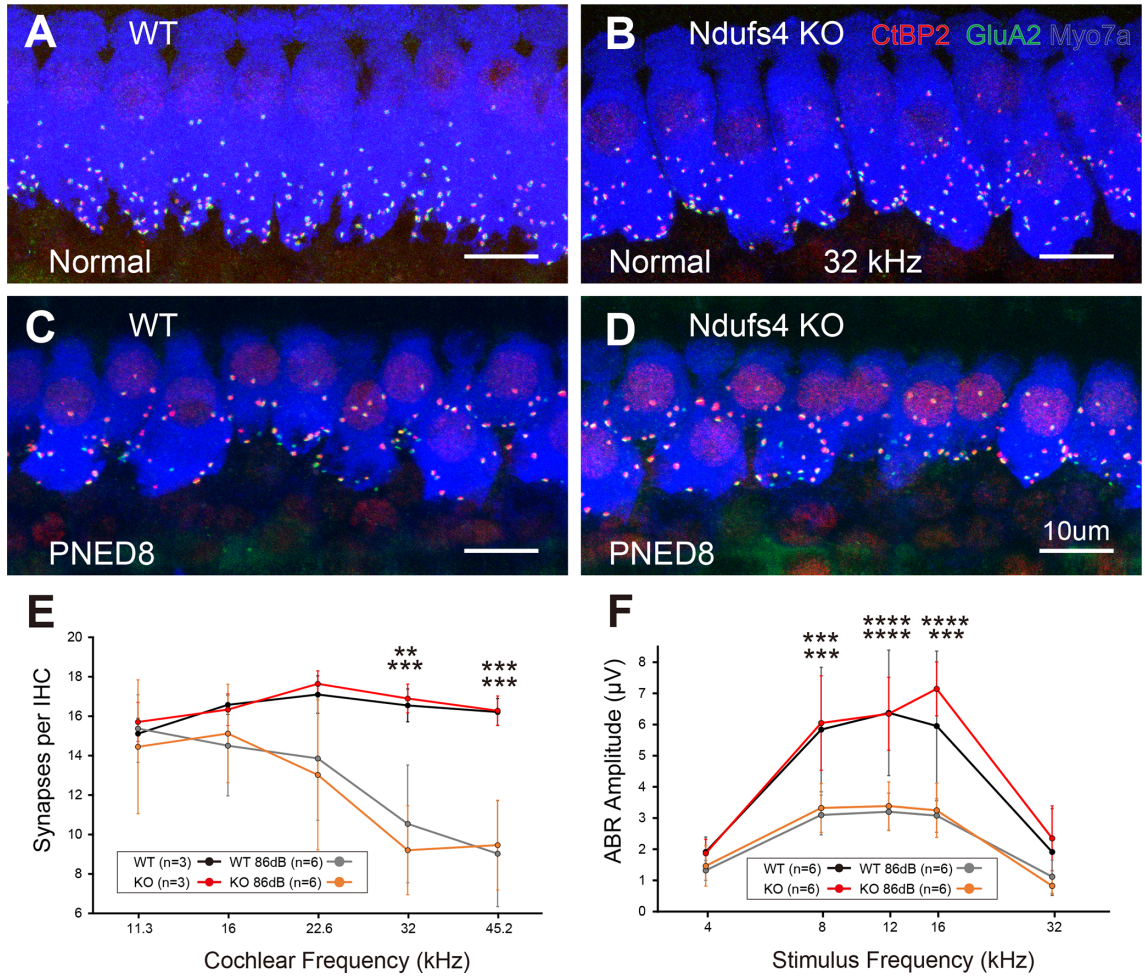

Fig. 4. Evaluation of inner hair cell synapses and auditory brainstem response (ABR) wave 1 amplitudes after mild noise exposure.
Maximum projection images of the inner hair cells (IHCs) of wild-type (WT) and *Ndufs4* knockout (KO) mice without noise exposure (A, B), and IHCs of WT and *Ndufs4* KO mice on post-86-dB-noise-exposure day 8 (PNED8) (C, D). Although 86 dB noise exposure caused significant loss of synaptic ribbons and functional synapses at the 32 and 45.2 kHz regions, there were no significant differences between WT and *Ndufs4* KO mice (E). The ABR wave 1 amplitudes were also attenuated at the 8, 12, and 16 kHz regions in both groups on PNED8, but there were no significant differences between WT and *Ndufs4* KO mice (F). Scale bars represent 10 μm (A-D). Statistical significance was determined by two-way analysis of variance, followed by a Šídák multiple comparison test. **P < 0.01; ***P < 0.001; ****P < 0.0001. Error bars represent the standard deviation.

KO mice compared with that in WT mice as previously reported (Chen et al. 2017; Shil et al. 2021).

Discussion

This study investigated Ndufs4 expression in the cochlea and explored whether *Ndufs4* deficiency causes vulnerability to various noise exposures. The findings of this study showed that Ndufs4 is broadly expressed in cochlea cells—IHCs, SGNs, and fibrocytes—and that *Ndufs4* deletion accelerates low-frequency PTS after severe noise exposure. On the other hand, significant differences were not observed in the number of IHC-SGN synapses after mild noise exposure. These results suggest that *Ndufs4* deficiency partly causes vulnerability to severe noise exposure causing PTS, but not to mild noise exposure.

Ndufs4 is one of the subunits in mitochondrial complex I and participates in the assembly and stability of complex I (Ingraham et al. 2009). A previous study (Kayser et al. 2016) revealed that *Ndufs4* deletion reduces maximum complex I-dependent oxidative phosphorylation in the synaptosomal mitochondria of the mouse brain stem, cerebellum, and olfactory bulb. Moreover, Ndufs4 is equally expressed in neurons, astrocytes, and oligodendrocytes in the hippocampus and cerebral cortex. A mitochondrial complex I respiration assay using isolated mitochondria from punch-out hippocampus of *Ndufs4* KO mice showed a significant decrease in basal respiration and maximal respiration in *Ndufs4* KO compared with WT (Shil et al. 2021). Considering that ubiquitous expression of Ndufs4 was

Table 1. The details of each description belonging to "generation of precursor metabolites and energy."

No.	Category	Term	Description	LogP	Genes
1	GO Biological Processes	GO:0006091	generation of precursor metabolites and energy	−3.36896	*ATP6, Ndufs4, Nr1d1, Eno1b*
2	GO Biological Processes	GO:0044057	regulation of system process	−3.27655	*Csrp3, Myl2, Ndufs4, Lmcd1, Eno1b*
3	GO Biological Processes	GO:0006163	purine nucleotide metabolic process	−3.23178	*ATP6, Ndufs4, Oas1a, Eno1b*
4	GO Biological Processes	GO:0046034	ATP metabolic process	−3.19546	*ATP6, Ndufs4, Eno1b*
5	GO Biological Processes	GO:0072521	purine-containing compound metabolic process	−3.08997	*ATP6, Ndufs4, Oas1a, Eno1b*

observed in the cochlea like in the hippocampus, mitochondrial complex I function is supposed to be similarly impaired in the cochlea of *Ndufs4* KO mice. The down-regulation of energy generation-related genes was confirmed through RNA sequencing, and this result supports our inference. However, measurements of the oxygen consumption rate using mouse cochlea tissues are still not established. Thus, future studies on this are warranted.

There was a significant elevation of low-tone hearing thresholds after severe noise exposure (100 dB) in *Ndufs4* KO mice. Although it is possible that a ceiling effect due to maximal hair cell injury mediated by *Ndufs4* deficiency prevented further threshold shifts in the higher frequency regions after noise exposure, we suspect this result reflects damage to various cells in the apical cochlear regions. Apparent differences were not observed between WT and *Ndufs4* KO mouse cochleae from the gross histological analyses, including the apical areas. Threshold shifts can be caused not only by hair cell loss but also by endolymphatic hydrops and stereocilia or strial damage (Hott et al. 2003; Kujawa and Liberman 2019). Therefore, low tone PTS in *Ndufs4* KO mice might be caused by cochlear mechanical or metabolic damage. Mitochondria are supposed to be involved in the metabolic damage and reactive oxygen species generation induced by noise trauma (Fujimoto and Yamasoba 2019), and noise exposure causes morphological changes to mitochondrial cristae in the OHCs of guinea pigs (Spoendlin 1971). Moreover, disruption of calcium ion regulation mediated by the mitochondria after noise exposure leads to mitochondria-mediated apoptosis (Vicente-Torres and Schacht 2006). Severe noise exposure can also cause vasoconstriction and ischemia of the cochlea, decreasing oxygen supplementation and ATP production accelerated by mitochondrial dysfunction (Quirk and Seidman 1995; Fujimoto and Yamasoba 2019). Noise vulnerability in *Ndufs4* KO mice is supposed to be mediated by these complex mechanisms of mitochondrial damage; however, the effect is limited in low-tone hearing. The difference in the mitochondrial distribution in different cochlear frequency regions has not been thoroughly studied yet. Given the fact that mitochondria are less prevalent and more asymmetric in the apical areas of the gerbil cochlea (Spicer and Schulte 1994), mitochondrial distribution and Ndufs4 function may differ depending on the region and influence the differences in noise sensitivity between cochlear regions. Differential gene expression along the cochlear frequency map of the mouse cochlea has been reported for various genes, such as receptors of γ-aminobutyric acid (Sato et al. 2009). Future studies evaluating mitochondrial characteristics, distribution, and the relationship with molecules that are differentially expressed at different cochlear frequency regions are needed.

Glutamate excitotoxicity is an instigating factor of cochlear synaptopathy (Liberman and Kujawa 2017). Excitotoxic noise can alter the ribbon size of auditory hair cells and cause hearing impairments (Liberman et al. 2015). In neuronal cells, glutamate excitotoxicity mechanisms are tightly related to mitochondrial function, and the key driver of the mechanism is an excessive increase in intracellular Ca^{2+} concentration (Plotegher et al. 2021). Similarly, the noise-dependent elevation of Ca^{2+} concentration is observed in cochlear sensory hair cells (Fridberger et al. 1998; Wang et al. 2018), and rapid Ca^{2+} entry into the mitochondrial matrix via the mitochondrial calcium uniporter occurs in turn (Chen et al. 2012). Recently, Wang et al. (2018) reported that cellular calcium influx during noise exposure leads to mitochondrial calcium overload via the mitochondrial calcium transporters including mitochondrial calcium uniporter, and mitochondrial calcium overload subsequently causes loss of not only hair cells but also synapses in mice. Moreover, Wong et al. (2019) showed that presynaptic Ca^{2+} influx and mitochondrial Ca^{2+} uptake couple in hair cells impacts synaptic ribbon formation and function in zebrafish. Although apparent differences in synapse numbers were not observed after noise exposure between WT and *Ndufs4* KO mice, this result does not deny the possibility that another mitochondrial dysfunction accelerates noise-induced cochlear synaptopathy. Nevertheless, the precise mitochondrial role in hair cell synapses remains unclear. Therefore, it will be interesting to expand the research using noise-induced cochlear synaptopathy models to the other mitochondrial dysfunction mouse models in the future.

This study has some limitations. First, although acoustic exposure is usually performed on adolescent or

adult mice at about 7-14 weeks of age, acoustic exposure was performed at 4 weeks because *Ndufs4* KO mice generally exhibit progressive hearing loss after 6 weeks of age and die around 7 weeks of age. Since noise exposure was performed during the developmental stage of hearing in this study, the effects of *Ndufs4* deficiency in adults are still unknown and may differ from the present results. In addition, the observation period after noise exposure was 8 days owing to the reason mentioned above; thus, the results of the final ABR measurement might have included TTS factors. Future studies using conditional KO mice of *Ndufs4* will be necessary to resolve this limitation. Second, the sample size was relatively small in this study owing to the rather low birth and survival rates of *Ndufs4* KO mice. However, we observed significant differences in various parameters; therefore, we think that the sample size was acceptable from the perspective of animal welfare. Third, because of the high possibility of death during the course of the experiments, we used the same sex mice (males or females) in each experiment to allow comparisons to be made even if some mice die. Although we must admit that sex differences may have influenced the experimental results, we do not expect these differences to be pronounced because our experiments were conducted at a stage not characterized by advanced sexual maturity. Fourth, we evaluated endolymphatic hydrops formation using cochlear samples with perilymph perfusion. Although apparent differences were not found between WT and *Ndufs4* KO mice, we must admit the possibility that the position of Reissner's membrane was affected by perilymph perfusion. Fifth, we used whole inner ear tissues for RNA sequencing. This method allows the evaluation of major changes in gene expression in tissues but not detailed changes in gene expression at the cellular level. In addition, we used P-values to obtain DEGs because DEGs selected based on false discovery rate were limited in this study. This means the accuracy of the RNA sequencing results is not high, and a single-cell RNA sequencing study is needed for a detailed evaluation in the future. Finally, although the down-regulation of energy generation-related genes in *Ndufs4* KO mouse cochlea was confirmed, mitochondrial functions such as the oxygen consumption rate could not be evaluated in this experiment because cochlear tissue is not as homogeneous and easily collected as brain or liver tissues. Complex I function is reduced by approximately half in the other tissues of *Ndufs4* KO mice; similar changes are expected in the cochlea. The establishment of a measurement method for cochlear mitochondrial function *in vivo* is a future challenge.

In conclusion, Ndufs4, a vital component of mitochondrial complex I, is broadly expressed in the cochlea. Moreover, *Ndufs4* deficiency accelerates threshold shifts of low frequency after severe noise exposure. However, this study did not evaluate the effect of *Ndufs4* deletion on age-related hearing loss, another representative sensory neural hearing loss like NIHL. Therefore, the relationship between Ndufs4 and sensorineural hearing loss is still unclear and requires further detailed studies.

Acknowledgments

We thank Dr. T. Sugasawa for contributing to the RNA sequencing and bioinformatics analysis and Ms. N. Shibata for contributing to the histological analyses. We thank Editage (https://www.editage.jp) for English language editing.

This work was supported by JSPS KAKENHI [grant numbers JP19K18792 (J.S.), JP22K09700 (J.S.), and JP20K22992 (K.H.)].

Author Contributions

J.S. and T.H. conceived the experiments. T.H. performed the experiments. Y.K., Y.H., R.I, K.H., C.S., T.K, T.A., Y.O., and Y.K. contributed to the materials. T.H. and J.S. performed analysis and interpretation of the data. Y.K. supervised the whole process. J.S. and T.H wrote the manuscript. All authors read and approved the final manuscript.

Conflict of Interest

The authors declare no conflict of interest.

References

Bolea, I., Gella, A., Sanz, E., Prada-Dacasa, P., Menardy, F., Bard, A.M., Machuca-Marquez, P., Eraso-Pichot, A., Modol-Caballero, G., Navarro, X., Kalume, F. & Quintana, A. (2019) Defined neuronal populations drive fatal phenotype in a mouse model of Leigh syndrome. *Elife*, **8**, e47163.

Chen, B., Hui, J., Montgomery, K.S., Gella, A., Bolea, I., Sanz, E., Palmiter, R.D. & Quintana, A. (2017) Loss of mitochondrial *Ndufs4* in striatal medium spiny neurons mediates progressive motor impairment in a mouse model of Leigh syndrome. *Front. Mol. Neurosci.*, **10**, 265.

Chen, Q., Mahendrasingam, S., Tickle, J.A., Hackney, C.M., Furness, D.N. & Fettiplace, R. (2012) The development, distribution and density of the plasma membrane calcium ATPase 2 calcium pump in rat cochlear hair cells. *Eur. J. Neurosci.*, **36**, 2302-2310.

Fridberger, A., Flock, A., Ulfendahl, M. & Flock, B. (1998) Acoustic overstimulation increases outer hair cell Ca^{2+} concentrations and causes dynamic contractions of the hearing organ. *Proc. Natl. Acad. Sci. U. S. A.*, **95**, 7127-7132.

Fujimoto, C. & Yamasoba, T. (2014) Oxidative stresses and mitochondrial dysfunction in age-related hearing loss. *Oxid. Med. Cell. Longev.*, **2014**, 582849.

Fujimoto, C. & Yamasoba, T. (2019) Mitochondria-targeted antioxidants for treatment of hearing loss: a systematic review. *Antioxidants* (*Basel, Switzerland*), **8**, 109.

Honkura, Y., Matsuo, H., Murakami, S., Sakiyama, M., Mizutari, K., Shiotani, A., Yamamoto, M., Morita, I., Shinomiya, N., Kawase, T., Katori, Y. & Motohashi, H. (2016) NRF2 is a key target for prevention of noise-induced hearing loss by reducing oxidative damage of cochlea. *Sci. Rep.*, **6**, 19329.

Honkura, Y., Suzuki, J., Sakayori, N., Inada, H., Kawase, T., Katori, Y. & Osumi, N. (2019) Effects of enriched endogenous omega-3 fatty acids on age-related hearing loss in mice. *BMC Res. Notes*, **12**, 768.

Hott, M.E., Graham, M., Bonassar, L.J. & Megerian, C.A. (2003) Correlation between hearing loss and scala media area in guinea pigs with long-standing endolymphatic hydrops. *Otol.*

Neurotol., **24**, 64-72.
Ingraham, C.A., Burwell, L.S., Skalska, J., Brookes, P.S., Howell, R.L., Sheu, S.S. & Pinkert, C.A. (2009) NDUFS4: creation of a mouse model mimicking a Complex I disorder. *Mitochondrion*, **9**, 204-210.
Kayser, E.B., Sedensky, M.M. & Morgan, P.G. (2016) Region-specific defects of respiratory capacities in the Ndufs4(KO) mouse brain. *PLoS One*, **11**, e0148219.
Kruse, S.E., Watt, W.C., Marcinek, D.J., Kapur, R.P., Schenkman, K.A. & Palmiter, R.D. (2008) Mice with mitochondrial complex I deficiency develop a fatal encephalomyopathy. *Cell Metab.*, **7**, 312-320.
Kujawa, S.G. & Liberman, M.C. (2009) Adding insult to injury: cochlear nerve degeneration after "temporary" noise-induced hearing loss. *J. Neurosci.*, **29**, 14077-14085.
Kujawa, S.G. & Liberman, M.C. (2019) Translating animal models to human therapeutics in noise-induced and age-related hearing loss. *Hear. Res.*, **377**, 44-52.
Lavinsky, J., Salehi, P., Wang, J. & Friedman, R.A. (2018) Genome-wide association study for noise-induced cochlear synaptopathy. *bioRxiv*, 311407.
Liberman, L.D., Suzuki, J. & Liberman, M.C. (2015) Dynamics of cochlear synaptopathy after acoustic overexposure. *J. Assoc. Res. Otolaryngol.*, **16**, 205-219.
Liberman, M.C. (2017) Noise-induced and age-related hearing loss: new perspectives and potential therapies. *F1000Res.*, **6**, 927.
Liberman, M.C. & Kujawa, S.G. (2017) Cochlear synaptopathy in acquired sensorineural hearing loss: manifestations and mechanisms. *Hear. Res.*, **349**, 138-147.
Ohlemiller, K.K., Wright, J.S. & Dugan, L.L. (1999) Early elevation of cochlear reactive oxygen species following noise exposure. *Audiol. Neurootol.*, **4**, 229-236.
Ortigoza-Escobar, J.D., Oyarzabal, A., Montero, R., Artuch, R., Jou, C., Jimenez, C., Gort, L., Briones, P., Muchart, J., Lopez-Gallardo, E., Emperador, S., Pesini, E.R., Montoya, J., Perez, B., Rodriguez-Pombo, P., et al. (2016) Ndufs4 related Leigh syndrome: a case report and review of the literature. *Mitochondrion*, **28**, 73-78.
Plotegher, N., Filadi, R., Pizzo, P. & Duchen, M.R. (2021) Excitotoxicity revisited: mitochondria on the verge of a nervous breakdown. *Trends Neurosci.*, **44**, 342-351.
Quintana, A., Kruse, S.E., Kapur, R.P., Sanz, E. & Palmiter, R.D. (2010) Complex I deficiency due to loss of Ndufs4 in the brain results in progressive encephalopathy resembling Leigh syndrome. *Proc. Natl. Acad. Sci. U. S. A.*, **107**, 10996-11001.
Quirk, W.S. & Seidman, M.D. (1995) Cochlear vascular changes in response to loud noise. *Am. J. Otol.*, **16**, 322-325.
Ruel, J., Wang, J., Rebillard, G., Eybalin, M., Lloyd, R., Pujol, R. & Puel, J.L. (2007) Physiology, pharmacology and plasticity at the inner hair cell synaptic complex. *Hear. Res.*, **227**, 19-27.
Sato, T., Doi, K., Hibino, H. & Kubo, T. (2009) Analysis of gene expression profiles along the tonotopic map of mouse cochlea by cDNA microarrays. *Acta Otolaryngol. Suppl.*, **129**, 12-17.
Schaette, R. & McAlpine, D. (2011) Tinnitus with a normal audiogram: physiological evidence for hidden hearing loss and computational model. *J. Neurosci.*, **31**, 13452-13457.
Shil, S.K., Kagawa, Y., Umaru, B.A., Nanto-Hara, F., Miyazaki, H., Yamamoto, Y., Kobayashi, S., Suzuki, C., Abe, T. & Owada, Y. (2021) Ndufs4 ablation decreases synaptophysin expression in hippocampus. *Sci. Rep.*, **11**, 10969.
Someya, S. & Prolla, T.A. (2010) Mitochondrial oxidative damage and apoptosis in age-related hearing loss. *Mech. Ageing Dev.*, **131**, 480-486.
Spicer, S.S. & Schulte, B.A. (1994) Differences along the place-frequency map in the structure of supporting cells in the gerbil cochlea. *Hear. Res.*, **79**, 161-177.
Spoendlin, H. (1971) Primary structural changes in the organ of Corti after acoustic overstimulation. *Acta Otolaryngol.*, **71**, 166-176.
Sterky, F.H. & Larsson, N.G. (2008) Complex I: a complex gateway to the powerhouse. *Cell Metab.*, **7**, 278-279.
Suzuki, J., Corfas, G. & Liberman, M.C. (2016) Round-window delivery of neurotrophin 3 regenerates cochlear synapses after acoustic overexposure. *Sci. Rep.*, **6**, 24907.
Suzuki, J., Inada, H., Han, C., Kim, M.J., Kimura, R., Takata, Y., Honkura, Y., Owada, Y., Kawase, T., Katori, Y., Someya, S. & Osumi, N. (2020) "Passenger gene" problem in transgenic C57BL/6 mice used in hearing research. *Neurosci. Res.*, **158**, 6-15.
Tuerdi, A., Kinoshita, M., Kamogashira, T., Fujimoto, C., Iwasaki, S., Shimizu, T. & Yamasoba, T. (2017) Manganese superoxide dismutase influences the extent of noise-induced hearing loss in mice. *Neurosci. Lett.*, **642**, 123-128.
Vicente-Torres, M.A. & Schacht, J. (2006) A BAD link to mitochondrial cell death in the cochlea of mice with noise-induced hearing loss. *J. Neurosci. Res.*, **83**, 1564-1572.
Wang, X., Zhu, Y., Long, H., Pan, S., Xiong, H., Fang, Q., Hill, K., Lai, R., Yuan, H. & Sha, S.H. (2018) Mitochondrial calcium transporters mediate sensitivity to noise-induced losses of hair cells and cochlear synapses. *Front. Mol. Neurosci.*, **11**, 469.
Wong, H.C., Zhang, Q., Beirl, A.J., Petralia, R.S., Wang, Y.X. & Kindt, K. (2019) Synaptic mitochondria regulate hair-cell synapse size and function. *Elife*, **8**, e48914.
Yamashita, D., Jiang, H.Y., Schacht, J. & Miller, J.M. (2004) Delayed production of free radicals following noise exposure. *Brain Res.*, **1019**, 201-209.
Zhou, Y., Zhou, B., Pache, L., Chang, M., Khodabakhshi, A.H., Tanaseichuk, O., Benner, C. & Chanda, S.K. (2019) Metascape provides a biologist-oriented resource for the analysis of systems-level datasets. *Nat. Commun.*, **10**, 1523.

Supplementary Files

Please find supplementary file(s);
https://doi.org/10.1620/tjem.2023.J031